5-9-2018

Methylglyoxal Uptake Coefficients on Aqueous Aerosol Surfaces

David O. De Haan
University of San Diego, ddehaan@sandiego.edu

Natalie G. Jimenez
University of San Diego

Alexia de Loera
University of San Diego

Mathieu Cazaunau

Aline Gratien

See next page for additional authors

Methylglyoxal Uptake Coefficients on Aqueous Aerosol Surfaces

Abstract

In order to predict the amount of secondary organic aerosol formed by heterogeneous processing of methylglyoxal, uptake coefficients (γ) and estimates of uptake reversibility are needed. Here, uptake coefficients are extracted from chamber studies involving ammonium sulfate and glycine seed aerosol at high relative humidity (RH ≥ 72%). Methylglyoxal uptake coefficients on prereacted glycine aerosol particles had a strong dependence on RH, increasing from $\gamma = 0.4 \times 10^{-3}$ to 5.7×10^{-3} between 72 and 99% RH. Continuous methylglyoxal losses were also observed in the presence of aqueous ammonium sulfate at 95% RH ($\gamma_{AS,wet} = 3.7 \pm 0.8 \times 10^{-3}$). Methylglyoxal uptake coefficients measured at ≥95% RH are larger than those reported for glyoxal on nonacidified, aqueous aerosol surfaces at 90% RH. Slight curvature in first-order uptake plots suggests that methylglyoxal uptake onto aqueous aerosol surfaces is not entirely irreversible after 20 min. Methylglyoxal uptake by cloud droplets was rapid and largely reversible, approaching equilibrium within the 1 min mixing time of the chamber. PTR-MS measurements showed that each cloud event extracted 3 to 8% of aerosol-phase methylglyoxal and returned it to the gas phase, likely by an oligomer hydrolysis mechanism.

Disciplines

Physical Chemistry

Author(s)

David O. De Haan, Natalie G. Jimenez, Alexia de Loera, Mathieu Cazaunau, Aline Gratien, Edouard Pangui, and Jean-Francois Doussin

Methylglyoxal Uptake Coefficients on Aqueous Aerosol Surfaces

David O. De Haan,[1] Natalie G. Jimenez,[1] Alexia de Loera,[1] Mathieu Cazaunau,[2] Aline Gratien,[2] Edouard Pangui,[2] Jean-François Doussin[2]*

[1]Department of Chemistry and Biochemistry, University of San Diego, 5998 Alcala Park, San Diego CA 92110 USA

[2]Laboratoire Interuniversitaire des Systèmes Atmosphériques (LISA), UMR CNRS 7583, Université Paris-Est-Créteil (UPEC) et Université Paris Diderot (UPD), Institut Pierre Simon Laplace (IPSL), Créteil, France

* Corresponding author contact: 011-1-619-260-6882, -011-1-619-260-2211 fax, ddehaan@sandiego.edu

ABSTRACT: In order to predict the amount of secondary organic aerosol formed by heterogeneous processing of methylglyoxal, uptake coefficients (γ) and estimates of uptake reversibility are needed. Here, uptake coefficients are extracted from chamber studies involving ammonium sulfate and glycine seed aerosol at high relative humidity (RH ≥72%). Methylglyoxal uptake coefficients on pre-reacted glycine aerosol particles had a strong dependence on RH, increasing from $\gamma = 0.4 \times 10^{-3}$ to 5.7×10^{-3} between 72 and 99% RH. Continuous methylglyoxal losses were also observed in the presence of aqueous ammonium sulfate at 95% RH ($\gamma_{AS,wet} = 3.7 \pm 0.8 \times 10^{-3}$). Methylglyoxal uptake coefficients measured at ≥95% RH are larger than those reported for glyoxal on non-acidified, aqueous aerosol surfaces at 90% RH. Slight curvature in 1st-order uptake plots suggests that methylglyoxal uptake onto aqueous aerosol surfaces is not entirely irreversible after 20 min. Methylglyoxal uptake by cloud droplets was rapid and largely reversible, approaching equilibrium within the 1 min mixing time of the chamber. PTR-MS measurements showed that each cloud event extracted 3 to 8% of aerosol-phase methylglyoxal and returned it to the gas phase, likely by an oligomer hydrolysis mechanism.

1. Introduction

Several studies have estimated the global amount of secondary organic aerosol formed from glyoxal and methylglyoxal via aqueous phase processes. These estimates range from 3 – 13 TgC/year for glyoxal[1-3] and 1.5 – 8 TgC/year for methylglyoxal.[2-4] Because the surface area and water content of clouds is much larger than that of aqueous aerosol particles, SOA production from dicarbonyls is assumed to take place predominantly in clouds.[3] These estimates of SOA production represent significant fractions of total SOA loading in some urban areas,[5] and have stimulated intense interest in the aqueous chemistry responsible for converting volatile carbonyl species into hydrate, oligomer, and acid products that can remain in the condensed phase after the cloud droplet evaporates. In addition, gas-phase reactions with water vapor or water clusters can convert aldehydes to diols,[6-9] blue-shifting their absorbance spectra,[9] lowering their vapor pressure, and making transfer to clouds and aerosol more likely.

Unfortunately, aqueous SOA production estimates for aldehydes are quite uncertain, given questions about the reversibility of uptake, the mechanism of uptake (dependent on surface area or ion catalysis),[10] and the magnitude of the uptake coefficient (γ) itself. Glyoxal uptake coefficients measurements have ranged from $\gamma = 1 \times 10^{-3}$ on aqueous droplets[11] to a photochemically enhanced uptake of $\gamma = 16 \times 10^{-3}$ on non-hygroscopic ammonium sulfate / fulvic acid aerosol.[10, 12] Glyoxal uptake coefficients have been found to depend on aerosol acidity,[13] relative humidity,[13-14] and ionic strength.[15] While the value of Liggio *et al.*[13] ($\gamma = 2.9 \times 10^{-3}$ on non-acidified aerosol) is most commonly used in modeling studies,[3, 16-17] high-end values ($\gamma = 16 \times 10^{-3}$) have been successfully used to model $PM_{2.5}$ levels in Mexico City.[5]

For methylglyoxal, the situation is even more uncertain. To our knowledge, methylglyoxal uptake coefficient has been reported only on 55-85% H_2SO_4 solutions.[18] Modeling studies have

adopted glyoxal uptake coefficients for methylglyoxal based on chemical similarity,[3, 5, 16-17] even though the two molecules are very different in important aspects such as surface activities,[19-21] hydration equilibrium constants,[22-23] Henry's law coefficients,[22-26] and oligomerization processes.[27-28] There is a clear need for measurements of methylglyoxal uptake coefficients onto aerosol and droplet surfaces that have atmospheric relevance. In this study, we extract methylglyoxal uptake coefficients from a series of chamber experiments performed on atmospherically relevant inorganic and organic seed aerosol at high relative humidity levels.

2. Materials and Methods

Experimental methods have been described earlier,[29] and will be only briefly described here. The CESAM 4.2 m^3 temperature-controlled chamber[30-31] uses input flows of humidified or dry purified air to offset sample flows and maintain constant pressure just above ambient levels. The stirred chamber, whose walls are uncoated 304L stainless steel, is pumped down to a few mTorr between each experiment, and cleaned with pure ethanol (VWR, 99%) and ultrapure water (18.2 MΩ, ELGA Maxima) between each set of experiments to remove contaminants. Chamber RH, measured to ± 2% (Vaisala HMP234 HUMICAP), was increased in discrete steps up to supersaturation by additions of high purity water vapor from a steel boiler.

Methylglyoxal solution samples (Alfa-Aesar) were pumped and stirred periodically to remove as much water as possible. The resulting brown viscous liquid was heated to produce green methylglyoxal gas (and a small, variable amount of water vapor) in a glass bulb at known pressure. Bulb contents were then transferred into the chamber using dry N_2. Ammonium sulfate (AS) and glycine seed aerosol particles were used as model particles for inorganic and organic aerosol, respectively, since AS is a common aerosol salt species and glycine is the most abundant amino acid in atmospheric aerosol. [32-33] Both species are reactive towards

methylglyoxal.[21, 34] Seed aerosol were produced by atomizing aqueous solutions of 1 – 2 mM AS or 10 mM glycine. AS droplets were diffusion-dried before being sent into a dry chamber. For glycine aerosol (Expt. 4), in order to generate a complex, atmospherically relevant surface containing oligomers and more functional groups than just carboxylic acids and amines, deliquesced glycine aerosol were "pre-reacted" with 1.0 ppm methylglyoxal and 0.68 ppm methylamine at 72% RH for 90 minutes before methylglyoxal concentrations was increased to 6.9 ppm and its uptake measured. Aerosol and cloud droplet size distributions were respectively monitored by SMPS (TSI 3080/3772, 20-900 nm, sampling via Nafion drying tube) and droplet scattering spectrometer (Welas, Palas Particle Tech., 0.25 to 15 μm, corrected for inlet losses[35]). Methylglyoxal gas concentrations in the chamber were calibrated using long-path FTIR (Bruker Tensor, calibration Figure S1, integrated methylglyoxal band intensity = 6.3×10^{-18} cm^2 $molecule^{-1}$ from 2720 to 2940 cm^{-1})[36] and monitored by PTR-MS (KORE Tech. Series II) through a 60 °C sampling line. Fast PTR-MS response to methylglyoxal additions (≤ 1 min. chamber mixing time) indicated no significant partitioning of methylglyoxal to the sampling line.

The uptake coefficient γ is the fraction of collisions of a gas molecule with a surface that lead to reactive uptake. The observed uptake coefficient, γ_{obs}, is calculated using eq. 1,

$$\gamma_{obs} = \frac{4k}{\bar{c}\,SA} \quad (1)$$

where k is the 1st-order rate constant (s^{-1}) extracted from the decay of gas-phase methylglyoxal signals after RH-dependent wall losses were subtracted, SA is the SMPS-measured surface area of aerosol (m^2 surface / m^3 air) or other surface, and c-bar is the mean speed of methylglyoxal molecules in m/s,

$$\bar{c} = \sqrt{\frac{8RT}{\pi M}} \quad (2)$$

97 where R = 8.3145 J $mol^{-1}K^{-1}$, T is temperature (Kelvin), and M is the molecular mass of
98 methylglyoxal (0.072 kg/mol). Stated uncertainties in uptake coefficients include experimental
99 uncertainties in wall loss rates, aerosol surface areas, and 1^{st}-order fits. The observed uptake
100 coefficient can be limited by gas-phase diffusion, mass accommodation, and/or reactivity and
101 diffusion in the condensed phase.[37] In this study, gas-phase diffusion was not the primary
102 limitation on observed uptake coefficients at RH ≤ 98%. At 99% RH, gas-phase diffusion
103 limitations likely suppressed the observed uptake coefficient by ~50%.

104 **3. Results**

105 Methylglyoxal concentrations measured by PTR-MS as a function of time in the chamber are
106 shown in Figure 1. Extracted first-order decay rate constants, aerosol or cloud surface areas, and
107 uptake coefficients are summarized in Table 1.

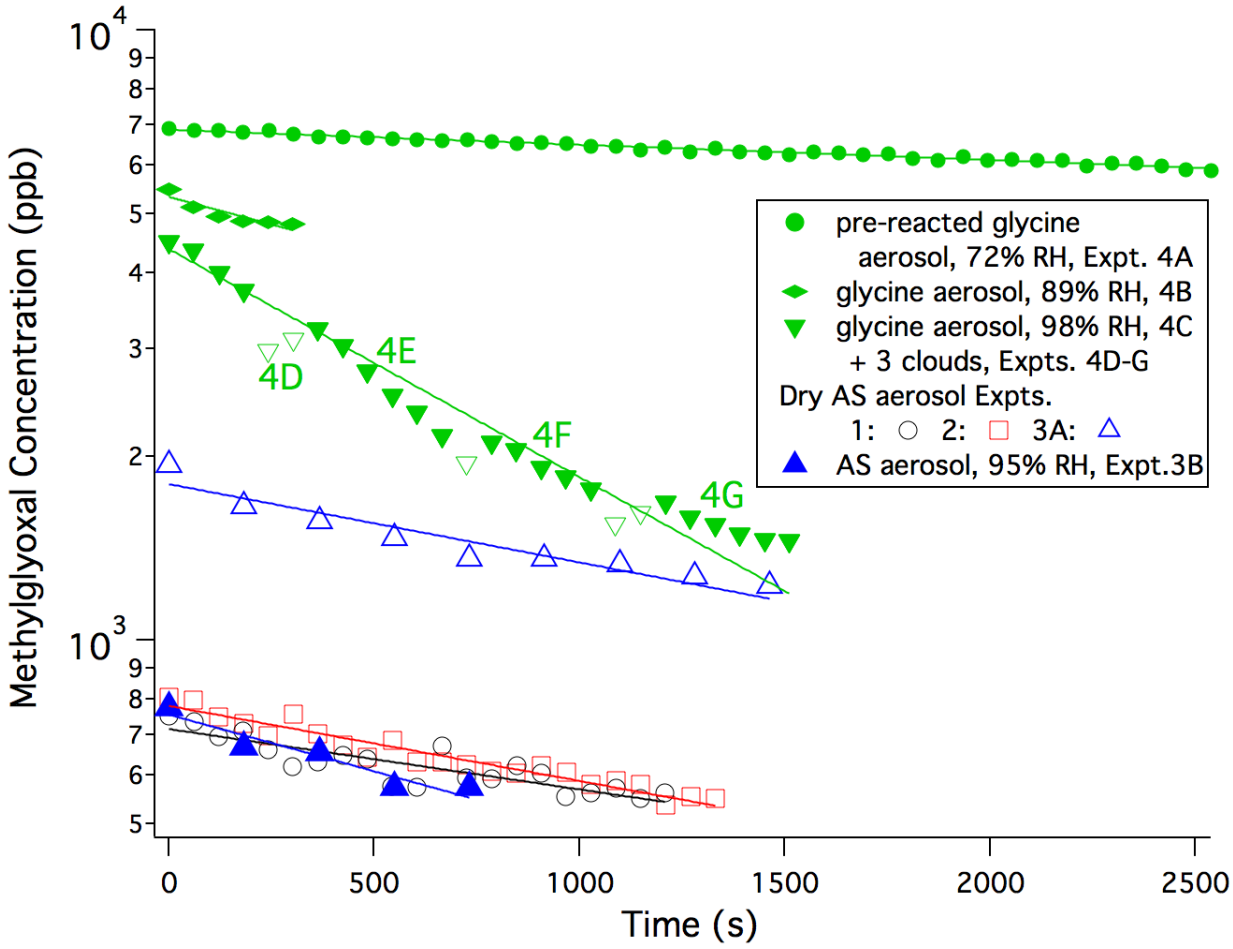

Figure 1: Methylglyoxal loss rates measured by PTR-MS, corrected for RH-dependent zero-order wall losses and sampling dilution in the constant-pressure CESAM chamber. Open symbols: dry chamber containing crystalline AS aerosol particles (black, Expt. 1; red, Expt. 2; blue, Expt. 3). Blue filled triangles (Expt. 3): chamber at 95 ±2% RH containing deliquesced AS aerosol. Green circles, diamonds, triangles (Expt. 4): chamber at 72, 89, and 98 ± 2% RH, respectively, containing deliquesced, pre-reacted glycine aerosol (exposed to 1.0 ppm methylglyoxal and 0.68 ppm methylamine at 72% RH for 90 min. before methylgyoxal concentration was increased to 6.9 ppm for uptake measurements at 72% RH). Expts. 4A, 4B, and 4C were performed sequentially. Green open triangles show three brief drops corresponding to three cloud events with RH > 100%; fit omits these data points. Expt 4C data is subdivided into labeled sections 4D (cloud 1) and 4E-4G (post-cloud 1-3, respectively).

Table 1: Measured Methylglyoxal Uptake Rate Constants and Uptake Coefficients

expt.	surface	% RH (± 2%)	$k_{surface}$ (10^{-4} s^{-1})[a]	surface area (10^{-3} m^2/m^3)	$\gamma_{surface}$ (10^{-3})
1	AS	< 5	< 2.3 ± 0.3	0.6 [b]	< 4.6 ± 0.6
2	AS	< 5	< 2.8 ± 0.2	0.7 [b]	< 4.7 ± 0.3
3A	AS	< 5	< 3.0 ± 0.4	1.0 [b]	< 3.5 ± 0.4
3B	AS	95	4.3 ± 0.8	1.6 [b]	3.7 ± 0.8
4A	glycine	72	0.62 ± 0.08	2.3 [c]	0.37 ± 0.06
4B	glycine	89	4.2 ± 1.1	2.5 [c]	2.3 ± 0.6
4C	glycine	98	8.6 ± 0.9	4.2 [c]	2.8 ± 0.4
4D	cloud droplet	> 100	> 17	80 – 500 [c]	d
4E	cloud-processed glycine	~99	11.0 ± 1.1	2.3 [c]	6.6 ± 1.0
4F	cloud-reprocessed glycine	~99	6.9 ± 0.8	1.7 [c]	5.7 ± 0.9
4G	cloud-reprocessed glycine	~99	4.5 ± 0.8	1.3 [c]	4.8 ± 1.0

a: Data corrected using measured RH-dependent zero-order wall losses: 0.018 ±0.007 ppb s^{-1} at < 5% RH, 0.09 ±0.03 ppb s^{-1} at 72% RH, and 0 ppb s^{-1} above 85% RH, where no net wall losses were observed due to equilibrium. **b**: SMPS aerosol particle surface area. **c**: WELAS aerosol particle surface area. **d**: Uptake not measurable because equilibrium achieved in <1 min.

3.1 Wall losses. Because the chamber has a surface area to volume ratio of ~4.3 m^2/m^3,[30] while aerosol in the chamber have < 0.003 m^2/m^3 total surface area, it is critical that the uptake of methylglyoxal onto the steel chamber walls be well-characterized so that wall and aerosol surface processes can be distinguished. Fourteen methylglyoxal wall loss experiments were therefore conducted at various concentrations (35 ppb to 2.5 ppm) and RH levels (0 to 87%). Measured 1st-order wall loss rate constants are shown in Figure S2. Measured 1st order wall loss rate constants varied by a factor of 300 and showed a large, negative dependence on methylglyoxal concentrations. In other words, steel chamber walls appear to take up methylglyoxal at a nearly constant rate that is independent of methylglyoxal concentrations,

suggesting that under our experimental conditions methylglyoxal losses on the steel chamber surfaces are limited by available surface uptake sites. In fact, we estimate that ~6×10^{19} methylglyoxal molecules, equivalent to 0.6 ppm in the CESAM chamber, would create a monolayer if adsorbed on the steel chamber walls. This is near the concentration median of our wall loss experiments, suggesting that competition for wall surface uptake sites could contribute to the lower uptake rate constants observed in higher concentration runs.

The near-constant wall losses observed are better expressed as zero-order loss rates, shown as a function of RH in Figure S3. Nine measurements at RH <15% were within a factor of 2 of each other, with an average methylglyoxal loss rate of 0.018 ±0.007 ppb s^{-1}. Five loss rate measurements on two other days were higher by factors of 8.4 ±0.5 and 33 (not shown in Figure S3). In the latter case, chamber walls were known to be contaminated with ammonium sulfate aerosol from earlier experiments. Thus, we take 0.018 ±0.007 ppb s^{-1} as the loss rate of methylglyoxal on clean and dry steel surfaces.

As relative humidity increases, the gas-phase reaction between methylglyoxal and water vapor converts more methylglyoxal to its hydrated diol form.[7, 9] Because the diol form of methylglyoxal is less volatile, losses of methylglyoxal to surfaces are expected to increase, and this is observed for wall losses in Figure S3 between 15 and 50% RH. However, at high RH, enhanced uptake rates are offset by hydrolysis of wall-deposited methylglyoxal oligomers,[29] rapidly establishing a gas/surface equilibrium similar to that observed in glyoxal chamber experiments.[13, 15] For example, when the relative humidity was increased from 0 to 87 ± 2% in a chamber experiment without seed particles, the gas-phase concentration of methylglyoxal increased by a factor of 2.6 and reached equilibrium within 2 min, twice the chamber mixing time. After this, methylglyoxal signals were quite stable over the next hour as the RH declined

159 from 87 to 82 ± 2%, rising an additional ~8% (perhaps due to the contribution of a slow dimer
160 hydrolysis process).[38] Similar observations were made when the chamber contained wall-
161 deposited aerosol. We thus conclude that at RH ≥ 85%, methylglyoxal rapidly equilibrates with
162 the steel chamber walls, because no net wall uptake is observed beyond 2 min. Thus, no
163 correction for wall loss is made in methylglyoxal experiments at RH ≥ 85%, while between 15
164 and 85% RH (*i.e.*, for Expt. 4A only), we estimate wall loss corrections using a 3rd-order
165 polynomial fit to the wall loss measurements plotted vs. RH (Figure S3).

166 3.2 Dry AS aerosol (Expts 1 – 3A). Figure 1 shows loss rates measured by PTR-MS in 3
167 experiments after methylglyoxal was added to the dry chamber containing AS aerosol particles
168 (open symbols). After correcting the data for wall losses on clean and dry steel (0.018 ±0.007
169 ppb s^{-1}), 1st order loss rate constants were calculated, and were found to increase with AS surface
170 areas, as expected (Table 1). The experiments show good consistency, with calculated uptake
171 coefficients $\gamma_{AS,dry}$ averaging (4.3 ±0.) $\times 10^{-3}$. This is an upper limit, however, because all 3
172 experiments were conducted with AS aerosol from previous experiments deposited on the walls,
173 and total observed loss rates were similar to maximum wall loss rates measured with wall-
174 deposited AS aerosol). Thus, wall-deposited AS aerosol may have contributed significantly to
175 observed methylglyoxal losses.

176 3.3 Deliquesced AS aerosol (Expt. 3B). Figure 1 also shows methylglyoxal uptake recorded
177 in the presence of AS aerosol immediately after the chamber RH increased from 79 to 95 ±2%
178 RH (filled blue triangles). This RH increase reached and exceeded the deliquescence point of the
179 previously dried AS aerosol, 80.6% RH,[39] forming aqueous droplets. The loss rate of
180 methylglyoxal observed over the next 12 min by PTR-MS corresponds to a 1st-order rate
181 constant $k = (4.3 \pm 0.8) \times 10^{-4}$ s^{-1}. This loss rate could be due to increased methylglyoxal uptake

by the deliquesced aerosol particles or by the chamber walls at higher RH. However, 25 min earlier, when the relative humidity of the seeded chamber was first increased to 79 ± 2%, the gas-phase methylglyoxal PTR-MS signals responded just as they did in the seed-free chamber: methylglyoxal signals stabilized within 3 min after a fast initial rise, with only a slight subsequent increase as RH levels dropped a few percent. This suggests that methyglyoxal rapidly reached equilibrium with the humid walls long before the second RH increase from 79 to 95 ± 2%. While the methylglyoxal wall equilibrium may have been perturbed by the second RH increase, unless this wall equilibrium takes much longer to establish itself at 95 ± 2% RH than at 79 or 87 ± 2% RH, it cannot explain the continuous 12-min decline observed in gas-phase methylglyoxal signals. Methylglyoxal uptake onto newly deliquesced seed particles is a more likely explanation of this signal decline.

The uptake coefficient from this methylglyoxal loss can be estimated given the uptake surface areas. The AS aerosol size distribution in the 95 ± 2% RH chamber was measured after drying to 62 ± 4% RH in the sampling line, due to a 7°C temperature differential between the cooled chamber and the room temperature SMPS. This RH change should cause deliquesced AS particles to shrink in diameter by a factor of 1.64 due to water loss.[40] The measured SMPS size distribution at 62% RH was therefore multiplied by a growth factor of 1.64, resulting in an estimated chamber aerosol surface area at 95 ± 2% RH of 1.58×10^{-3} m^2/m^3. The methylglyoxal uptake coefficient onto deliquesced AS aerosol is then $\gamma = (3.7 \pm 0.8) \times 10^{-3}$.

3.4 Deliquesced glycine aerosol (Expt. 4A - C). After deliquesced glycine aerosol, 0.68 ppm methylamine, and 1.0 ppm methylglyoxal equilibrated in the chamber for 90 min. at 72 ± 2% RH, additional methylglyoxal was injected into the chamber to reach 6.9 ppm. Starting 10 min later when PTR-MS data collection commenced, constant methylglyoxal losses were observed

for 40 min (Figure 1, Expt. 4A). The RH-dependent wall loss function shown in Figure S3 was used to estimate the methylglyoxal wall loss rate at 72 ± 2% RH to be 0.09 ± 0.03 ppb s^{-1}, which was 5× lower than the observed total methylglyoxal loss rate, and resulted in a calculated first order loss constant k of $(6.2 \pm 0.8) \times 10^{-5}$ s^{-1}. The aerosol size distribution could be measured in this experiment by both SMPS (dried) and droplet scattering spectrometer (wet). After these two datasets were corrected for changes in RH during sampling and droplet losses in the inlet, respectively, the surface areas measured by the two techniques agreed to within 16%. The uptake coefficient is then $\gamma = (0.37 \pm 0.06) \times 10^{-3}$. We attribute this lower uptake to the fact that the deliquesced glycine aerosol particles had already reacted with ≥1.0 ppm methylglyoxal and 0.68 ppm methylamine in the chamber for a total of 100 min. before the methylglyoxal uptake rate was measured. At 72 ± 2% RH, the mole fraction of water in non-effloresced glycine aerosol particles is 41%,[41] and the water mass fraction is therefore only 14%. These meta-stable, non-crystalline glycine seed particles may be quite viscous, such that surface "aging" is possible and an aged surface may persist for hours.

When the RH was increased to 89 ± 2%, water content in the glycine seed aerosol should increase to 22% by mass,[41] reducing particle viscosity. This RH increase caused methylglyoxal loss rates to increase more than 5-fold to $k = (4.2 \pm 1.1) \times 10^{-4}$ s^{-1} (Figure 1, Expt. 4B). No change was observed in the methylamine gas concentration measured by PTR-MS or the surface area of the fully dried aerosol measured by SMPS. Since methylamine concentrations did not change, it is unlikely that methylglyoxal + methylamine reactions are the cause of the increased methylglyoxal losses. The increase in methylglyoxal uptake rate is more likely due to increased glycine aerosol surface area at higher RH. Surface area was estimated to be $(2.5 \pm 0.1) \times 10^{-3}$ m^2/m^3 using both hygroscopic growth corrected SMPS data and droplet spectrometer data

corrected for inlet losses (agreement to within 5%). The measured methylglyoxal uptake corresponds to an uptake coefficient of $\gamma = (2.3 \pm 0.6) \times 10^{-3}$ for aqueous glycine aerosol at 89 ±2% RH.

When the RH was increased to near saturation (98 ± 2% RH, Expt. 4C), the rate of methylglyoxal losses more than doubled again to $k = (8.6 \pm 0.9) \times 10^{-4}$ s^{-1}. The effect of 3 intervening cloud events is discussed below, and cloud data points are omitted in the present analysis. Near H_2O saturation, correcting SMPS measurements of dried aerosol with hygroscopic growth factors introduces large uncertainties, so droplet spectrometer measurements of wet particle surface area are more accurate. The addition of water vapor to increase RH from 89 to 98 ± 2% caused an increase in wet aerosol surface area to $(4.2 \pm 0.4) \times 10^{-3}$ m^2/m^3, resulting in a methylglyoxal uptake coefficient on aqueous glycine aerosol surfaces of $\gamma = (2.8 \pm 0.4) \times 10^{-3}$. The similarity of this value to the uptake coefficient on aqueous AS aerosol at 95 ± 2% RH ($\gamma = (3.7 \pm 0.8 \times 10^{-3})$ increases confidence in the analysis.

Figure 1 shows that the fit to methylglyoxal concentration data with cloud data points removed is also a reasonable fit for the pre-cloud data (glycine aerosol at 98 ± 2% RH). In fact, if only the four pre-cloud data points are used to calculate a methylglyoxal uptake coefficient, the result is within 11% of the previously calculated uptake coefficient. However, it is also apparent from Figure 1 that methylglyoxal loss rates decline after each cloud event. Fitting each of these slopes separately and using the droplet spectrometer surface areas measured after each cloud event allows estimates to be made of methylglyoxal uptake by "cloud-processed" glycine aerosol just below the saturation point (99 ± 1% RH). These estimates (Table 1, Expts. 4E – G) show that methylglyoxal uptake rates decline with decreasing aerosol surface area, resulting in an average uptake coefficient of $\gamma = (5.7 \pm 1.0) \times 10^{-3}$ for cloud-processed glycine at 99 ± 1% RH.

3.5 Cloud droplets (Expt. 4D). Figure 2 shows methylglyoxal PTR-MS signals and droplet spectrometer size distributions and total droplet counts recorded during three cloud events in Expt. 4. Each cloud event caused gas-phase methyglyoxal signals to decline initially, and then to recover after a few minutes as the cloud dissipated, evidence of reversible uptake of methylglyoxal by cloud droplets. These brief excursions in the methylglyoxal signals, which occur at the rate of chamber mixing (~1 min), are superimposed on a longer-term loss trend that we attribute to uptake on aqueous glycine aerosol particles and have already analyzed above. The size of the brief decline caused by each cloud event is proportional to the peak cloud droplet counts (Figure S4). Furthermore, because cloud droplet size distributions are initially similar, methylglyoxal declines are also roughly proportional to peak cloud droplet surface areas. While the 1-min time resolution of the data is clearly inadequate to follow this fast and reversible process in detail, the first cloud event caused a 760 ppb drop in methylglyoxal concentrations within 1 min, which would produce an in-cloud methylglyoxal concentration of 54 mM given the maximum total cloud droplet volume of 2.5 mL for this cloud event. Since the gas phase concentration after this uptake is 3.0 ppm, this corresponds to an effective Henry's law coefficient of 1.8×10^4 M atm^{-1} at 27 °C, significantly above previously reported values (3710 ± 320 M atm^{-1} at 25 °C).[24] This suggests that in these cloud events, the long-term declining trend obscures the magnitude of the cloud effect, and that some of the observed methylglyoxal uptake during cloud events is likely to the walls.) It appears that gas / cloud droplet equilibrium is reached in < 1 min. for methylglyoxal, and uptake coefficients onto cloud surfaces can therefore not be resolved by this experiment due to the slower (~1 min.) chamber mixing times.

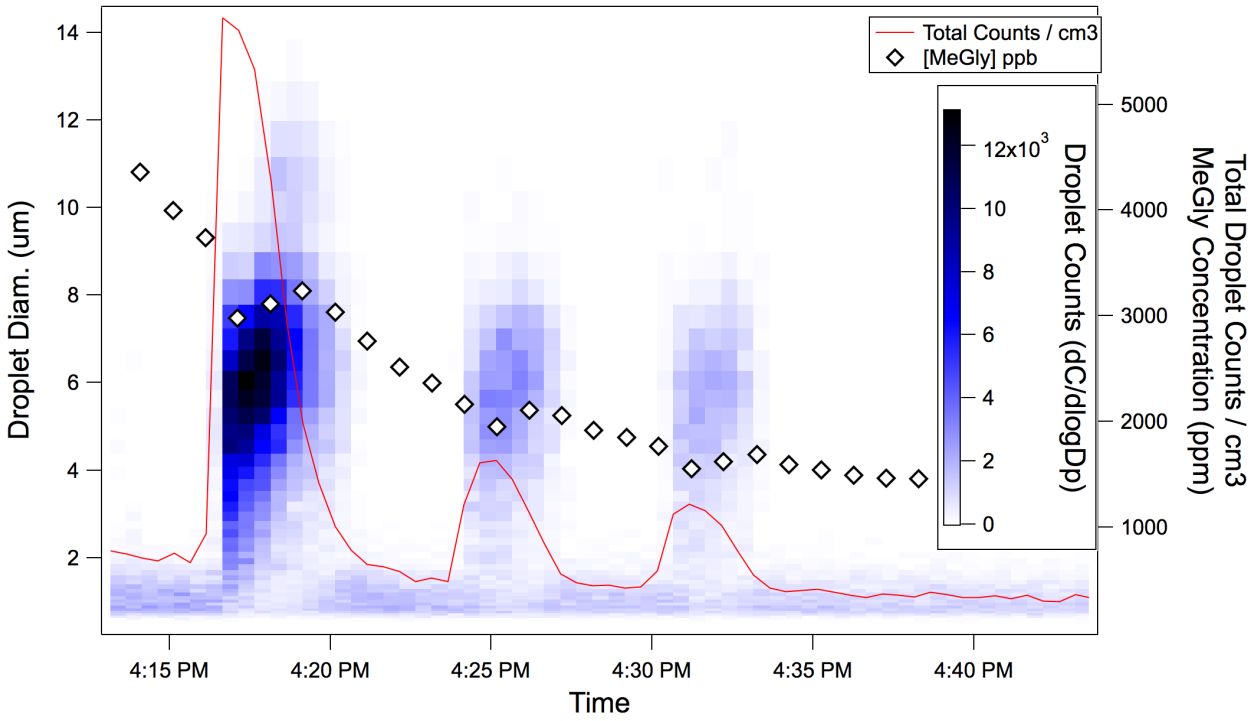

Figure 2: Glycine aerosol activation and reversible uptake of methylglyoxal by 3 clouds (Expt. 4). Blue color scale: cloud droplet spectra (30 s averaging, counts at each diameter size bin (left axis) vs. time). Red line: total droplet counts, corrected for inlet losses[35] (right axis). Open diamonds: PTR-MS methylglyoxal concentrations in ppb measured by PTR-MS (black diamonds, right axis).

4. Discussion

Figure 3 compares glyoxal uptake measurements on non-acidified (AS and sodium nitrate) aerosol surfaces reported by Liggio *et al.*[13] with our methylglyoxal uptake measurements on aqueous AS and pre-reacted glycine seeds as a function of relative humidity. While glyoxal uptake to non-acidifed aerosol does not appear to depend on RH, methylglyoxal uptake to pre-reacted glycine is strongly RH dependent, increasing by a factor of 15 between 72 and 99% RH. If we assume that glyoxal uptake coefficients are constant above 90% RH, in this range methylglyoxal uptake by aqueous aerosol surfaces is more efficient than glyoxal uptake. This is unexpected, since glyoxal has a higher effective Henry's law coefficient, especially in the presence of AS. The measured methylglyoxal uptake coefficient on cloud-processed glycine at

289 99% RH is also a factor of 2 larger than the $\gamma_{glyoxal}$ = 2.9 $\times 10^{-3}$ value used for methylglyoxal
290 uptake to cloud droplets in some recent modeling studies.[3, 17]

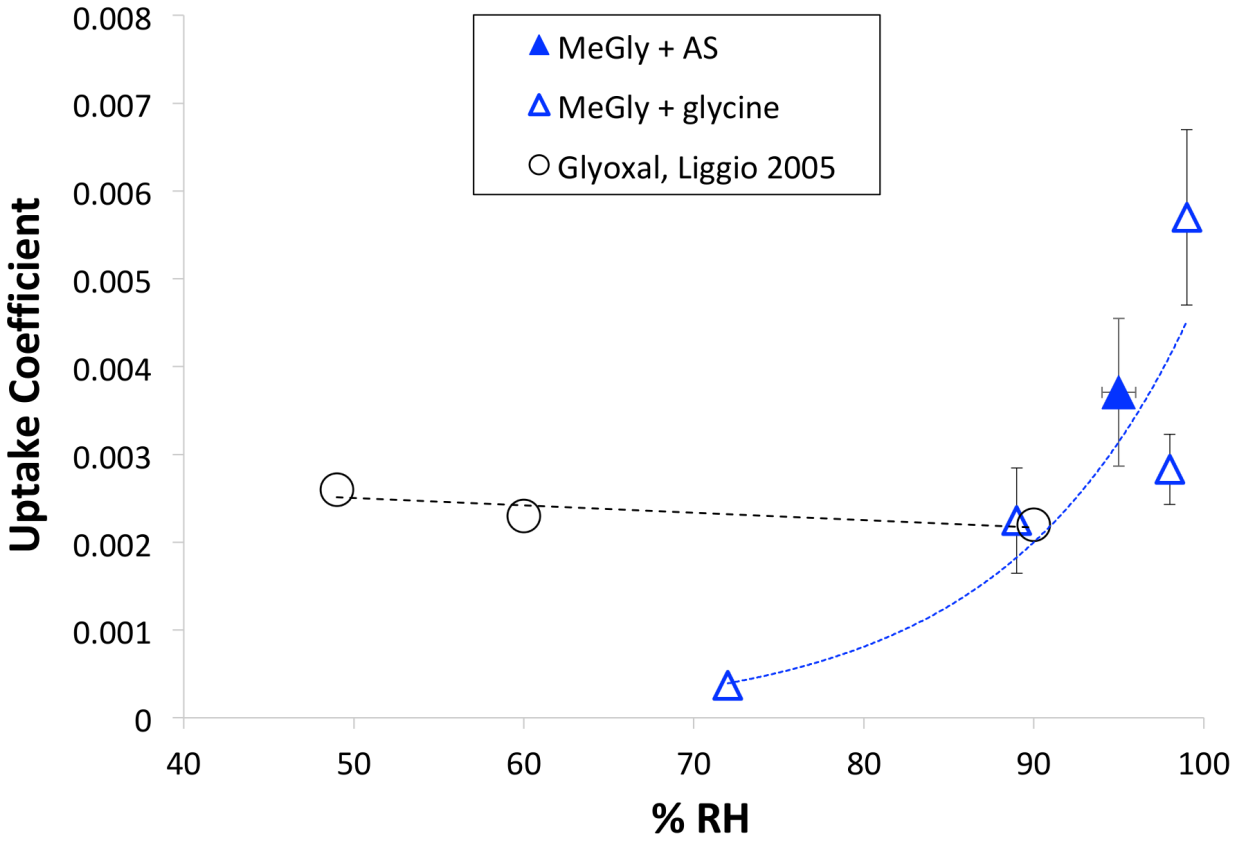

291
292 Figure 3: Comparison of measured uptake coefficients on non-acidified aerosol measured for
293 methylglyoxal (blue filled triangle, AS; blue open triangles, pre-reacted glycine aerosol) and
294 glyoxal (black open circles, AS and sodium nitrate aerosol, from ref [13])

295 The observation from Figure 2 that uptake of methylglyoxal into cloud droplets is largely
296 reversible is consistent with droplet evaporation measurements, which showed that ~80% of the
297 methylglyoxal in a droplet consistently evaporated along with the water, even when ammonium
298 salts were present.[4] Thus, treating methylglyoxal uptake to clouds as an irreversible process will
299 overestimate organic aerosol production by methylglyoxal in clouds by a factor of 5.

300 It is also important to note that the methyglyoxal PTRMS signals in Figure 2 recorded after
301 each cloud event are higher than would be predicted from extrapolation of the pre-cloud signals

in each case. This is especially obvious after the second cloud event at 4:25 pm. These post-cloud increases in methylglyoxal gas concentrations indicate that cloud droplets do more than take up methylglyoxal reversibly. The cloud droplets also appear to return to the gas phase a fraction of the methylglyoxal that had previously been taken up by the aqueous glycine aerosol particle that nucleated the droplet. The addition of abundant water to the aerosol particle upon cloud nucleation likely hydrolyzes some methyglyoxal oligomers, adding to the monomer pool, some of which dehydrate and return to the gas phase in order to reestablish equilibrium. This hydrolytic loss of particle-phase methylglyoxal can evidently outpace hydration and deposition of gas-phase methylglyoxal, even though the latter process is enhanced at high RH.[7, 9]

Fitting the methylglyoxal data before each cloud event and extrapolating to the first three after-cloud measurements, we estimated the increase in methylglyoxal gas produced by each cloud relative to the expectation from the previous trend, and compared these increases to the total methylglyoxal taken up previously by aqueous glycine aerosol. The result is that cloud events 1 and 2 each returned 7.9 ± 1.2 % and cloud event 3 returned 3.4 ± 0.3 % of previously absorbed aerosol-phase methylglyoxal back to the gas phase. In other words, approximately 20% of the total aqueous methylglyoxal SOA produced in this experiment was hydrolyzed during cloud processing back into methylglyoxal gas. Thus, even if methylglyoxal uptake appeared to be fully irreversible based on an aerosol experiment, subsequent cloud processing can retroactively change this conclusion.

Some reversibility in uptake of methylglyoxal to aqueous aerosol is also implied by the slight curvature beyond the first-order fits that can be seen in Figure 1. While methylglyoxal uptake onto glycine aerosol particles at 72 ± 2% RH shows no visible curvature over 40 min, all data collected with AS or glycine aerosol at RH ≥ 89% show some curvature. This may indicate that

methylglyoxal is being released from more diluted aqueous aerosol particles at rates that are detectably increasing during the 15 – 25 min duration of these measurements.

5. Conclusion

Uptake coefficients of methylglyoxal onto aqueous glycine and AS aerosol particles were found to be similar in magnitude, increasing with RH up to $(5.7 \pm 0.9) \times 10^{-3}$ at 99 ± 1% RH. This maximum uptake coefficient is a factor of 2 larger than the one (borrowed from glyoxal measurements) most commonly used in modeling studies of methylglyoxal uptake to clouds and aqueous aerosol. In this work, methylglyoxal uptake during cloud events was rapid and reversible, reaching equilibrium within the 1 min. mixing time of the chamber, and so precluding calculation of uptake coefficients onto cloud droplets. Gas phase methyglyoxal concentrations after cloud events were higher than predicted based on pre-cloud trends, indicating that each cloud event caused the volatilization of 3 to 8% of aerosol phase methylglyoxal, likely via oligomer hydrolysis. Finally, curvature in 1^{st}-order plots of methylglyoxal losses to aqueous aerosol particles at RH ≥ 89% suggests that some methylglyoxal is being released from aqueous aerosol to the gas phase. While equilibrium is not approached within 20 min., methylglyoxal uptake to aqueous aerosol is at least partially reversible at RH ≥ 89%.

Acknowledgments

This work was supported by NSF grant AGS-1523178. The authors thank V. Vaida for sharing critical methylglyoxal wall uptake data, R. Volkamer for helpful discussions, and acknowledge CNRS-INSU for supporting CESAM as an open facility through the National Instrument label. The CESAM chamber has received funding from the European Union's Horizon 2020 research and innovation programme through the EUROCHAMP-2020 Infrastructure Activity under grant agreement No 730997.

Supporting Information

The Supporting Information is available free of charge on the ACS Publications website.

Methylglyoxal calibration data, methylglyoxal wall losses graphed against methylglyoxal concentrations and relative humidity, and methylglyoxal losses during cloud events graphed against peak cloud droplet counts.

References

1. Stavrakou, T.; Müller, J.-F.; De Smedt, I.; Van Roozendael, M.; Kanakidou, M.; Vrekoussis, M.; Wittrock, F.; Richter, A.; Burrows, J. P., The continental source of glyoxal estimated by the synergistic use of spaceborne measurements and inverse modelling. *Atmos. Chem. Phys.* **2009,** *9*, 8431-8446.
2. Myriokefalitakis, S.; Tsigaridis, K.; Mihalopoulos, N.; Sciare, J.; Nenes, A.; Kawamura, K.; Segers, A.; Kanakidou, M., In-cloud oxalate formation in the global troposphere: a 3-D modeling study. *Atmos. Chem. Phys.* **2011,** *11*, 5761-5782.
3. Fu, T.-M.; Jacob, D. J.; Wittrock, F.; Burrows, J. P.; Vrekoussis, M.; Henze, D. K., Global budgets of atmospheric glyoxal and methylglyoxal, and implications for formation of secondary organic aerosols. *J. Geophys. Res.* **2008,** *113*, D15303.
4. Galloway, M. M.; Powelson, M. H.; Sedehi, N.; Wood, S. E.; Millage, K. D.; Kononenko, J. A.; Rynaski, A. D.; De Haan, D. O., Secondary organic aerosol formation during evaporation of droplets containing atmospheric aldehydes, amines, and ammonium sulfate. *Environ Sci Technol* **2014,** *48*, 14417-14425.
5. Ying, Q.; Cureño, I. V.; Chen, G.; Ali, S.; Zhang, H.; Malloy, M.; Bravo, H. A.; Sosa, R., Impacts of Stabilized Criegee Intermediates, surface uptake processes and higher aromatic secondary organic aerosol yields on predicted PM2.5 concentrations in the Mexico City Metropolitan Zone. *Atmos. Environ.* **2014,** *94*, 438-447.
6. Plath, K. L.; Axson, J. L.; Nelson, G. C.; Takahashi, K.; Skodje, R. T.; Vaidaa, V., Gas-phase vibrational spectra of glyoxylic acid and its gem diol monohydrate. Implications for atmospheric chemistry. *Reaction Kinetics and Catalysis Letters* **2009,** *96*, 209-224.
7. Axson, J. L.; Takahashi, K.; De Haan, D. O.; Vaida, V., Gas-phase water-mediated equilibrium between methylglyoxal and its geminal diol. *P. Natl. Acad. Sci. USA* **2010,** *107*, 6687-6692.
8. Kumar, M.; Francisco, J. S., The Role of Catalysis in Alkanediol Decomposition: Implications for General Detection of Alkanediols and Their Formation in the Atmosphere. *The Journal of Physical Chemistry A* **2015,** *119*, 9821-9833.
9. Kroll, J. A.; Hansen, A. S.; Møller, K. H.; Axson, J. L.; Kjaergaard, H. G.; Vaida, V., Ultraviolet Spectroscopy of the Gas Phase Hydration of Methylglyoxal. *ACS Earth and Space Chemistry* **2017,** *1*, 345-352.
10. Ervens, B.; Volkamer, R., Glyoxal processing by aerosol multiphase chemistry: towards a kinetic modeling framework of secondary organic aerosol formation in aqueous particles. *Atmos. Chem. Phys.* **2010,** *10*, 8219-8244.

11. Schweitzer, F.; Magi, L.; Mirabel, P.; George, C., Uptake rate measurements of methanesulfonic acid and glyoxal by aqueous droplets. *J. Phys. Chem.* **1998,** *102*, 593-600.
12. Volkamer, R.; Ziemann, P. J.; Molina, M. J., Secondary organic aerosol formation from acetylene (C_2H_2): seed effect on SOA yields due to organic photochemistry in the aerosol aqueous phase. *Atmos. Chem. Phys.* **2009,** *9*, 1907-1928.
13. Liggio, J.; Li, S.-M.; McLaren, R., Reactive uptake of glyoxal by particulate matter. *J. Geophys. Res.* **2005,** *110*, D10304.
14. Corrigan, A. L.; Hanley, S. W.; De Haan, D. O., Uptake of glyoxal by organic and inorganic aerosol. *Environ. Sci. Technol.* **2008,** *42*, 4428-4433.
15. Kroll, J. H.; Ng, N. L.; Murphy, S. M.; Varutbangkul, V.; Flagan, R. C.; Seinfeld, J. H., Chamber studies of secondary organic aerosol growth by reactive uptake of simple carbonyl compounds. *J. Geophys. Res.* **2005,** *110*, D23207.
16. Parikh, H. M.; Carlton, A. G.; Zhou, Y.; Zhang, H.; Kamens, R. M.; Vizuete, W., Modeling secondary organic aerosol formation from xylene and aromatic mixtures using a dynamic partitioning approach incorporating particle aqueous-phase chemistry (II). *Atmos. Environ.* **2012,** *56*, 250-260.
17. Li, J.; Cleveland, M.; Ziemba, L. D.; Griffin, R. J.; Barsanti, K. C.; Pankow, J. F.; Ying, Q., Modeling regional secondary organic aerosol using the Master Chemical Mechanism. *Atmos. Environ.* **2015,** *102*, 52-61.
18. Zhao, J.; Levitt, N. P.; Zhang, R.; Chen, J., Heterogeneous reactions of methylglyoxal in acidic media: implications for secondary organic aerosol formation. *Environ. Sci. Technol.* **2006,** *40*, 7682-7687.
19. Sareen, N.; Schwier, A. N.; Lathem, T. L.; Nenes, A.; McNeill, V. F., Surfactants from the gas phase may promote cloud droplet formation. *Proc. Natl. Acad. Sci. (USA)* **2013,** *110*, 2723-2728.
20. Shapiro, E. L.; Szprengiel, J.; Sareen, N.; Jen, C. N.; Giordano, M. R.; McNeill, V. F., Light-absorbing secondary organic material formed by glyoxal in aqueous aerosol mimics. *Atmos. Chem. Phys.* **2009,** *9*, 2289-2300.
21. Sareen, N.; Schwier, A. N.; Shapiro, E. L.; Mitroo, D.; McNeill, V. F., Secondary organic material formed by methylglyoxal in aqueous aerosol mimics. *Atmos. Chem. Phys.* **2010,** *10*, 997-1016.
22. Doussin, J. F.; Monod, A., Structure–activity relationship for the estimation of OH-oxidation rate constants of carbonyl compounds in the aqueous phase. *Atmos. Chem. Phys.* **2013,** *13*, 11625-11641.
23. Raventos-Duran, T.; Camredon, M.; Valorso, R.; Mouchel-Vallon, C.; Aumont, B., Structure-activity relationships to estimate the effective Henry's law constants of organics of atmospheric interest. *Atmos. Chem. Phys.* **2010,** *10*, 7643-7654.
24. Betterton, E. A.; Hoffmann, M. R., Henry's Law constants of some environmentally important aldehydes. *Environ. Sci. Technol.* **1988,** *22*, 1415-1418.
25. Ip, H. S. S.; Huang, X. H. H.; Yu, J. Z., Effective Henry's law constants of glyoxal, glyoxylic acid, and glycolic acid. *Geophys. Res. Lett.* **2009,** *36*, L01802.
26. Waxman, E. M.; Elm, J.; Kurtén, T.; Mikkelsen, K. V.; Ziemann, P. J.; Volkamer, R., Glyoxal and Methylglyoxal Setschenow Salting Constants in Sulfate, Nitrate, and Chloride Solutions: Measurements and Gibbs Energies. *Environ Sci Technol* **2015,** *49*, 11500-11508.
27. Kua, J.; Hanley, S. W.; De Haan, D. O., Thermodynamics and kinetics of glyoxal dimer formation: a computational study. *J. Phys. Chem.* **2008,** *112*, 66-72.

28. Krizner, H. E.; De Haan, D. O.; Kua, J., Thermodynamics and kinetics of methylglyoxal dimer formation: A computational study. *J. Phys. Chem.* **2009,** *113*, 6994-7001.
29. De Haan, D. O.; Hawkins, L. N.; Welsh, H. G.; Pednekar, R.; Casar, J. R.; Pennington, E. A.; de Loera, A.; Jimenez, N. G.; Symons, M. A.; Zauscher, M., *et al.*, Brown carbon production in ammonium- or amine-containing aerosol particles by reactive uptake of methylglyoxal and photolytic cloud cycling. *Environ Sci Technol* **2017,** *51*, 7458-7466.
30. Wang, J.; Doussin, J. F.; Perrier, S.; Perraudin, E.; Katrib, Y.; Pangui, E.; Picquet-Varrault, B., Design of a new multi-phase experimental simulation chamber for atmospheric photosmog, aerosol and cloud chemistry research. *Atmos. Meas. Tech.* **2011,** *4*, 2465-2494.
31. Denjean, C.; Formenti, P.; Picquet-Varrault, B.; Katrib, Y.; Pangui, E.; Zapf, P.; Doussin, J. F., A new experimental approach to study the hygroscopic and optical properties of aerosols: application to ammonium sulfate particles. *Atmos. Meas. Tech.* **2014,** *7*, 183-197.
32. Mopper, K.; Zika, R. G., Free amino acids in marine rains: evidence for oxidation and potential role in nitrogen cycling. *Nature* **1987,** *325*, 246-249.
33. Zhang, Q.; Anastasio, C., Free and combined amino compounds in atmospheric fine particles (PM2.5) and fog waters from Northern California. *Atmos. Environ.* **2003,** *37*, 2247-2258.
34. De Haan, D. O.; Hawkins, L. N.; Kononenko, J. A.; Turley, J. J.; Corrigan, A. L.; Tolbert, M. A.; Jimenez, J. L., Formation of nitrogen-containing oligomers by methylglyoxal and amines in simulated evaporating cloud droplets. *Environ. Sci. Technol.* **2011,** *45*, 984-991.
35. von der Weiden, S.-L.; Drewnick, F.; Borrmann, S., Particle Loss Calculator — a new software tool for the assessment of the performance of aerosol inlet systems. *Atmos. Meas. Tech.* **2009,** *2*, 479-494.
36. Eurochamp, Eurochamp-2: Integration of European Simulation Chambers for Investigating Atmospheric Processes. CEAM: Valencia, Spain, 2010.
37. Finlayson-Pitts, B. J.; Pitts, J. N., Jr., *Chemistry of the upper and lower atmosphere*. Academic Press: San Diego, 2000.
38. Fratzke, A. R.; Reilly, P. J., Thermodynamic and kinetic analysis of the dimerization of aqueous glyoxal. *Intl. J. Chem. Kinet.* **1986,** *18*, 775-789.
39. Zamora, I. R.; Tabazadeh, A.; Golden, D. M.; Jacobson, M. Z., Hygroscopic growth of common organic aerosol solutes, including humic substances, as derived from water activity measurements. *Journal of Geophysical Research: Atmospheres* **2011,** *116*, D23207
40. Topping, D. O.; McFiggans, G. B.; Coe, H., A curved multi-component aerosol hygroscopicity model framework: Part 1 – Inorganic compounds. *Atmos. Chem. Phys.* **2005,** *5*, 1205-1222.
41. Chan, M. N.; Choi, M. Y.; Ng, N. L.; Chan, C. K., Hygroscopicity of water-soluble organic compounds in atmospheric aerosols: amino acids and biomass derived organic species. *Environ. Sci. Technol.* **2005,** *39*, 1555-1562.

472 TOC artwork:

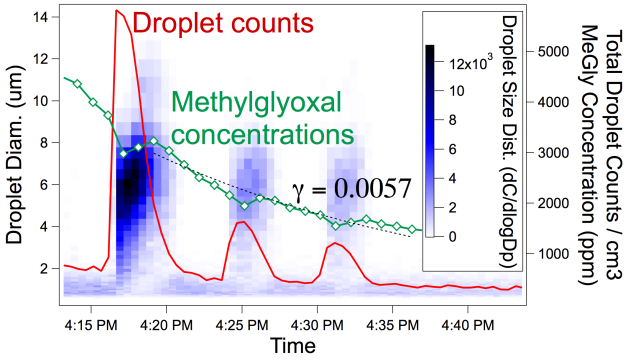

473

Supplemental Information:

Methylglyoxal Uptake Coefficients on Aqueous Aerosol Surfaces

David O. De Haan,[1] Natalie G. Jimenez,[1] Alexia de Loera,[1] Mathieu Cazaunau,[2] Aline Gratien,[2] Edouard Pangui,[2] Jean-François Doussin[2]*

[1]Department of Chemistry and Biochemistry, University of San Diego, 5998 Alcala Park, San Diego CA 92110 USA

[2]Laboratoire Interuniversitaire des Systèmes Atmosphériques (LISA), UMR CNRS 7583, Université Paris-Est-Créteil (UPEC) et Université Paris Diderot (UPD), Institut Pierre Simon Laplace (IPSL), Créteil, France

Corresponding author contact: 011-1-619-260-6882, 011-1-619-260-2211 fax, ddehaan@sandiego.edu

5 pages (including cover sheet)

Figures S1 – S4

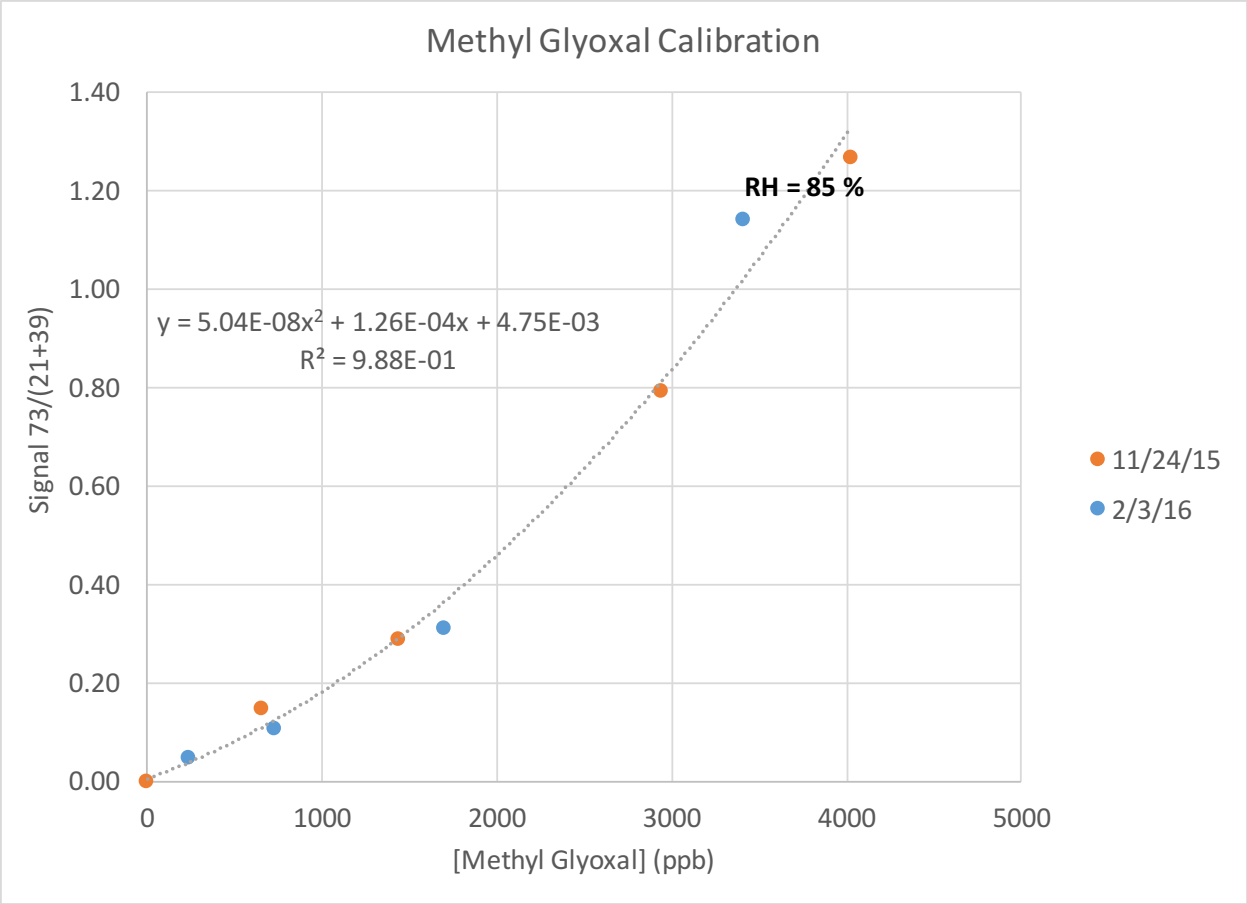

Figure S1: Calibration curve for water-corrected PTR-MS methylglyoxal signals vs concentrations in ppb based on FTIR absorbance bands.

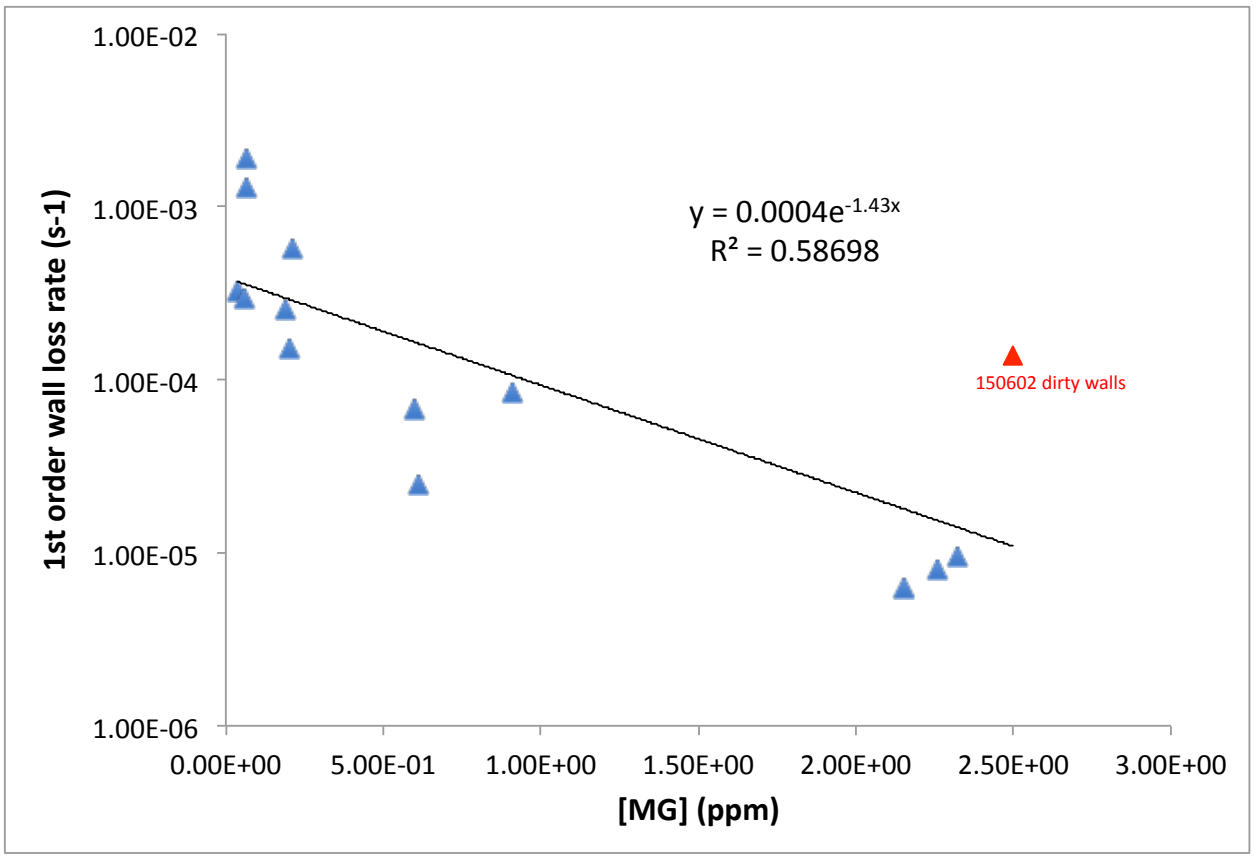

Figure S2: First order wall loss rates for methylglyoxal (s^{-1}) measured in dry (RH ≤ 15%), aerosol-free CESAM chamber as a function of methylglyoxal concentrations (ppm). First order wall loss rates varied by a factor of 300 and showed a dependence on [MeGly]. Red triangle denotes run where methylglyoxal wall uptake was measured in chamber that had been used for ammonium sulfate aerosol experiments for the previous week, such that wall uptake was likely enhanced by previously deposited AS aerosol. Other wall loss measurement runs (blue triangles) did not have significant quantities of aerosol particles deposited on the chamber walls.

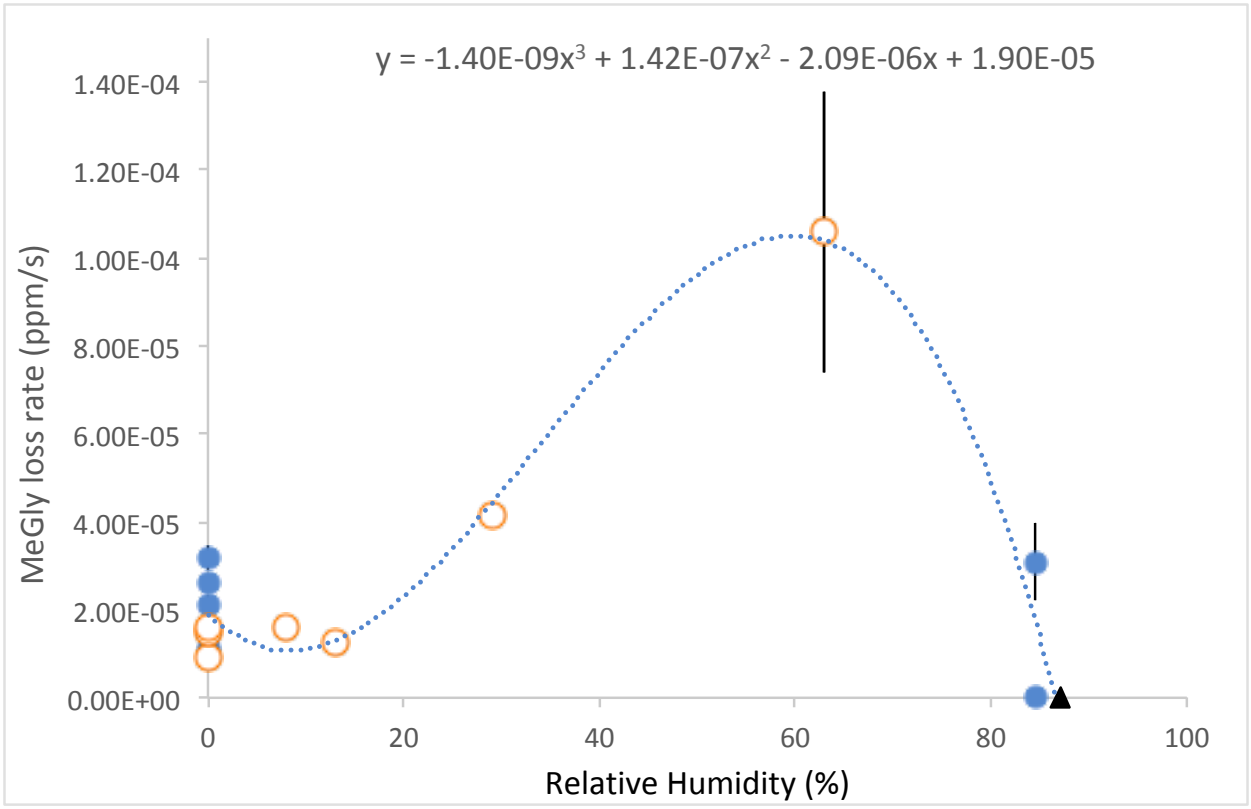

Figure S3: Zero order wall loss rates for methylglyoxal (in ppm s^{-1}) measured in aerosol-free CESAM chamber as a function of relative humidity. Different symbols denote data measured on different days. No data from experiments with wall-deposited aerosol is included.

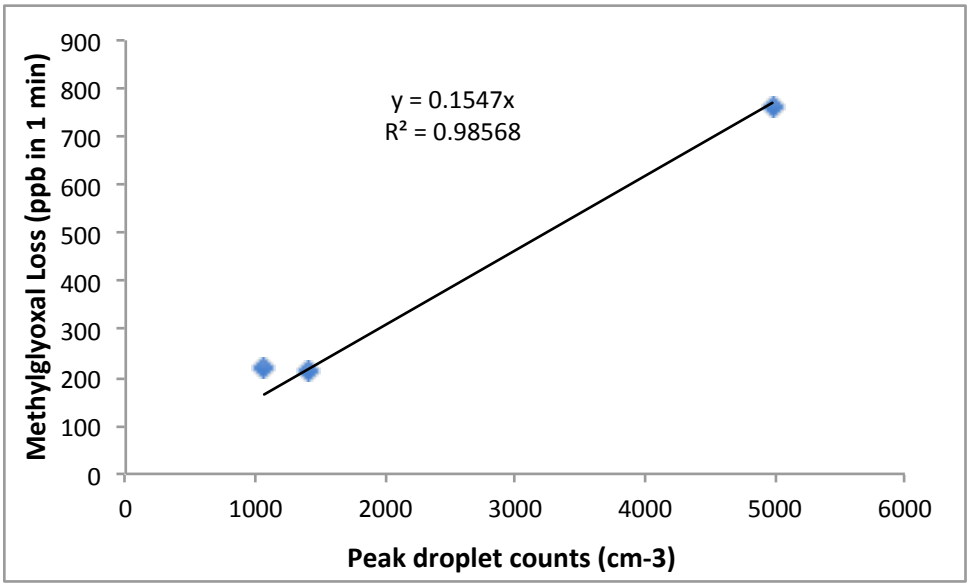

Figure S4: Methylglyoxal losses (in ppb) recorded by PTR-MS over 1 minute time step during three cloud events, graphed as a function of peak droplet counts recorded by droplet spectrometer. Pre-reacted glycine seed aerosol served as cloud condensation nuclei.